Graphic Anaesthesia

Essential diagrams, equations and tables for anaesthesia

OTHER TITLES FROM SCION

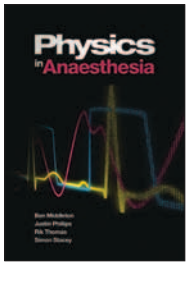

9781904842989

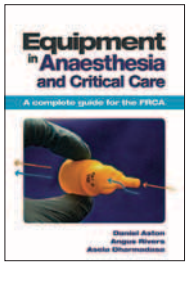

9781907904059

9781907904035

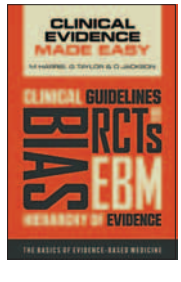

9781907904202

For more details see www.scionpublishing.com

Graphic Anaesthesia

Essential diagrams, equations and tables for anaesthesia

Dr Tim Hooper FRCA FFICM RAMC
Consultant in Intensive Care Medicine, Anaesthesia and Prehospital Care
Defence Medical Services, Southmead Hospital, Bristol

Dr James Nickells FRCA
Consultant in Anaesthesia
Southmead Hospital, Bristol

Dr Sonja Payne FRCA
Specialty Trainee in Anaesthesia
Severn Deanery

Dr Annabel Pearson FRCA
Specialty Trainee in Anaesthesia
Severn Deanery

Dr Benjamin Walton MRCP FRCA FFICM
Consultant in Intensive Care Medicine and Anaesthesia
Southmead Hospital, Bristol

Scion

© Scion Publishing Limited, 2015

First published 2015

All rights reserved. No part of this book may be reproduced or transmitted, in any form or by any means, without permission.

A CIP catalogue record for this book is available from the British Library.

ISBN 978 1 907904 33 2

Scion Publishing Limited

The Old Hayloft, Vantage Business Park, Bloxham Road, Banbury OX16 9UX, UK
www.scionpublishing.com

Important Note from the Publisher

The information contained within this book was obtained by Scion Publishing Ltd from sources believed by us to be reliable. However, while every effort has been made to ensure its accuracy, no responsibility for loss or injury whatsoever occasioned to any person acting or refraining from action as a result of information contained herein can be accepted by the authors or publishers.

Readers are reminded that medicine is a constantly evolving science and while the authors and publishers have ensured that all dosages, applications and practices are based on current indications, there may be specific practices which differ between communities. You should always follow the guidelines laid down by the manufacturers of specific products and the relevant authorities in the country in which you are practising.

Although every effort has been made to ensure that all owners of copyright material have been acknowledged in this publication, we would be pleased to acknowledge in subsequent reprints or editions any omissions brought to our attention.

Registered names, trademarks, etc. used in this book, even when not marked as such, are not to be considered unprotected by law.

Typeset by Medlar Publishing Solutions Pvt Ltd, India
Printed in the UK

Contents

Preface . . . xiii
About the authors . . . xiii
Abbreviations . . . xiv

SECTION 1 PHYSIOLOGY

1.1 Cardiac

1.1.1 Cardiac action potential – contractile cells . . . 1
1.1.2 Cardiac action potential – pacemaker cells . . . 2
1.1.3 Cardiac action potential – variation in pacemaker potential . . . 3
1.1.4 Cardiac cycle . . . 4
1.1.5 Cardiac output equation . . . 5
1.1.6 Central venous pressure waveform . . . 6
1.1.7 Central venous pressure waveform – abnormalities . . . 7
1.1.8 Einthoven triangle . . . 8
1.1.9 Ejection fraction equation . . . 9
1.1.10 Electrocardiogram . . . 10
1.1.11 Electrocardiogram – cardiac axis and QTc . . . 11
1.1.12 Fick method for cardiac output studies . . . 12
1.1.13 Frank–Starling curve . . . 13
1.1.14 Oxygen flux . . . 14
1.1.15 Pacemaker nomenclature – antibradycardia . . . 15
1.1.16 Pacemaker nomenclature – antitachycardia (implantable cardioverter defibrillators) . . . 16
1.1.17 Preload, contractility and afterload . . . 17
1.1.18 Pulmonary artery catheter trace . . . 18
1.1.19 Systemic and pulmonary pressures . . . 19
1.1.20 Valsalva manoeuvre . . . 20
1.1.21 Valsalva manoeuvre – clinical applications and physiological abnormalities . . . 21
1.1.22 Vaughan–Williams classification . . . 22
1.1.23 Ventricular pressure–volume loop – left ventricle . . . 23
1.1.24 Ventricular pressure–volume loop – right ventricle . . . 24

1.2 Circulation

1.2.1 Blood flow and oxygen consumption of organs . . . 25
1.2.2 Blood vessel structure . . . 26
1.2.3 Hagen–Poiseuille equation . . . 27
1.2.4 Laminar and turbulent flow . . . 28
1.2.5 Laplace's law . . . 29
1.2.6 Ohm's law . . . 30
1.2.7 Starling forces in capillaries . . . 31
1.2.8 Starling forces in capillaries – pathology . . . 32
1.2.9 Systemic vascular resistance . . . 33

1.3 Respiratory

1.3.1 Alveolar gas equation . . . 34
1.3.2 Alveolar partial pressure of oxygen and blood flow . . . 35
1.3.3 Bohr equation . . . 36
1.3.4 Carbon dioxide dissociation curve and Haldane effect . . . 37
1.3.5 Closing capacity . . . 38
1.3.6 Dead space and Fowler's method . . . 39
1.3.7 Diffusion . . . 40
1.3.8 Dynamic compression of airways . . . 41
1.3.9 Fick principle and blood flow . . . 42
1.3.10 Forced expiration curves . . . 43
1.3.11 Functional residual capacity of the lungs . . . 44
1.3.12 Lung and chest wall compliance . . . 45
1.3.13 Lung pressure–volume loop . . . 46
1.3.14 Lung volumes and capacities . . . 47
1.3.15 Oxygen cascade . . . 48
1.3.16 Oxygen dissociation curve and Bohr effect . . . 49
1.3.17 Pulmonary vascular resistance . . . 50
1.3.18 Pulmonary vascular resistance and lung volumes . . . 51
1.3.19 Respiratory flow–volume loops . . . 52
1.3.20 Shunt . . . 53
1.3.21 Ventilation–perfusion ratio . . . 54
1.3.22 Ventilatory response to carbon dioxide . . . 55
1.3.23 Ventilatory response to oxygen . . . 56
1.3.24 West lung zones . . . 57
1.3.25 Work of breathing . . . 58

1.4 Neurology

1.4.1 Action potential . . . 59
1.4.2 Cerebral blood flow and blood pressure . . . 60
1.4.3 Cerebral blood flow variation with ventilation . . . 61
1.4.4 Cerebrospinal fluid . . . 62
1.4.5 Gate control theory of pain . . . 63
1.4.6 Glasgow Coma Scale . . . 64
1.4.7 Intracranial pressure–volume relationship . . . 65
1.4.8 Intracranial pressure waveform . . . 66
1.4.9 Neuron . . . 67
1.4.10 Neurotransmitters – action . . . 68
1.4.11 Neurotransmitters – classification . . . 69
1.4.12 Reflex arc . . . 70
1.4.13 Synaptic transmission . . . 71
1.4.14 Types of nerve . . . 72
1.4.15 Visual pathway . . . 73

1.5 Renal

1.5.1 Autoregulation of renal blood flow . . . 74
1.5.2 Clearance . . . 75

1.5.3 Glomerular filtration rate . . . 76
1.5.4 Loop of Henle . . . 77
1.5.5 Nephron . . . 78
1.5.6 Renin–angiotensin–aldosterone system . . . 79

1.6 Gut
1.6.1 Bile . . . 80
1.6.2 Mediators of gut motility . . . 81

1.7 Acid–base
1.7.1 Acid–base disturbances . . . 82
1.7.2 Anion gap . . . 83
1.7.3 Buffer solution . . . 84
1.7.4 Dissociation constant and pKa . . . 85
1.7.5 Henderson–Hasselbalch equation . . . 86
1.7.6 Lactic acidosis . . . 87
1.7.7 pH . . . 88
1.7.8 Strong ion difference . . . 89

1.8 Metabolic
1.8.1 Krebs cycle . . . 90
1.8.2 Liver lobule . . . 91
1.8.3 Nutrition and energy . . . 92
1.8.4 Vitamins – sources and function . . . 93
1.8.5 Vitamins – toxicity and deficiency . . . 94

1.9 Endocrine
1.9.1 Adrenal gland . . . 95
1.9.2 Adrenergic receptor actions . . . 96
1.9.3 Catecholamine synthesis . . . 97
1.9.4 Hypothalamic–pituitary–adrenal axis – anatomy . . . 98
1.9.5 Hypothalamic–pituitary–adrenal axis – hormones . . . 99
1.9.6 Vitamin D synthesis . . . 100

1.10 Body fluids
1.10.1 Body fluid composition . . . 101
1.10.2 Fluid compartments . . . 102
1.10.3 Intravenous fluid composition . . . 103

1.11 Haematology
1.11.1 Antibody . . . 104
1.11.2 Blood groups . . . 105
1.11.3 Coagulation – cascade (classic) model . . . 106
1.11.4 Coagulation – cell-based model . . . 107
1.11.5 Complement cascade . . . 108
1.11.6 Haemoglobin . . . 109
1.11.7 Prostanoid synthesis . . . 110

1.12 Cellular
1.12.1 Cell . . . 111
1.12.2 Cell membrane . . . 112
1.12.3 G-proteins . . . 113
1.12.4 Ion channels . . . 114
1.12.5 Sodium/potassium–ATPase pump . . . 115

1.13 Muscle
1.13.1 Actin–myosin cycle . . . 116
1.13.2 Golgi tendon organ . . . 117
1.13.3 Muscle spindle . . . 118
1.13.4 Muscle types . . . 119
1.13.5 Neuromuscular junction . . . 120
1.13.6 Sarcomere . . . 121
1.13.7 Skeletal muscle structure . . . 122

SECTION 2 ANATOMY

2.1 Abdominal wall . . . 123
2.2 Antecubital fossa . . . 124
2.3 Autonomic nervous system . . . 125
2.4 Base of skull . . . 126
2.5 Brachial plexus . . . 127
2.6 Bronchial tree . . . 128
2.7 Cardiac vessels – cardiac veins . . . 129
2.8 Cardiac vessels – coronary arteries . . . 130
2.9 Circle of Willis . . . 131
2.10 Cranial nerves . . . 132
2.11 Cross-section of neck at C6 . . . 133
2.12 Cross-section of spinal cord . . . 134
2.13 Dermatomes . . . 135
2.14 Diaphragm . . . 136
2.15 Epidural space . . . 137
2.16 Femoral triangle . . . 138
2.17 Fetal circulation . . . 139
2.18 Intercostal space . . . 140
2.19 Internal jugular vein . . . 141
2.20 Laryngeal innervation . . . 142
2.21 Larynx . . . 143
2.22 Limb muscle innervation (myotomes) . . . 144
2.23 Lumbar plexus . . . 145
2.24 Nose . . . 146
2.25 Orbit . . . 147
2.26 Rib . . . 148
2.27 Sacral plexus . . . 149
2.28 Sacrum . . . 150
2.29 Spinal nerve . . . 151

2.30 Thoracic inlet and first rib 152
2.31 Vertebra 153

SECTION 3 PHARMACODYNAMICS AND KINETICS

3.1 Clearance 155
3.2 Compartment model – one and two compartments 156
3.3 Compartment model – three compartments 157
3.4 Dose–response curves 158
3.5 Elimination 159
3.6 Elimination kinetics 160
3.7 Half-lives and time constants 161
3.8 Meyer–Overton hypothesis 162
3.9 Volume of distribution 163
3.10 Wash-in curves for volatile agents 164

SECTION 4 DRUGS

4.1 Anaesthetic agents – etomidate 165
4.2 Anaesthetic agents – ketamine 166
4.3 Anaesthetic agents – propofol 167
4.4 Anaesthetic agents – thiopentone 168
4.5 Local anaesthetics – mode of action 169
4.6 Local anaesthetics – properties 170
4.7 Neuromuscular blockers – mode of action 171
4.8 Neuromuscular blocking agents – depolarizing 172
4.9 Neuromuscular blocking agents – non-depolarizing 173
4.10 Opioids – mode of action 174
4.11 Opioids – properties 175
4.12 Volatile anaesthetic agents – mode of action 176
4.13 Volatile anaesthetic agents – physiological effects 177
4.14 Volatile anaesthetic agents – properties 178

SECTION 5 PHYSICS

5.1 Avogadro's law 179
5.2 Beer–Lambert law 180
5.3 Critical temperatures and pressure 181
5.4 Diathermy 182
5.5 Doppler effect 183
5.6 Electrical safety 184
5.7 Electricity 185
5.8 Exponential function 186
5.9 Fick's law of diffusion 187
5.10 Gas laws – Boyle's law 188

5.11 Gas laws – Charles' law . . . 189
5.12 Gas laws – Gay-Lussac's (Third Perfect) law . . . 190
5.13 Gas laws – ideal gas law and Dalton's law . . . 191
5.14 Graham's law . . . 192
5.15 Heat . . . 193
5.16 Henry's law . . . 194
5.17 Humidity . . . 195
5.18 Laser . . . 196
5.19 Metric prefixes . . . 197
5.20 Power . . . 198
5.21 Pressure . . . 199
5.22 Raman effect . . . 200
5.23 Reflection and refraction . . . 201
5.24 SI units . . . 202
5.25 Triple point of water and phase diagram . . . 203
5.26 Types of flow . . . 204
5.27 Wave characteristics . . . 205
5.28 Wheatstone bridge . . . 206
5.29 Work . . . 207

SECTION 6 CLINICAL MEASUREMENT

6.1 Bourdon gauge . . . 209
6.2 Clark electrode . . . 210
6.3 Damping . . . 211
6.4 Fuel cell . . . 212
6.5 Monitoring of neuromuscular blockade . . . 213
6.6 Oximetry – paramagnetic analyser . . . 214
6.7 pH measuring system . . . 215
6.8 Pulse oximeter . . . 216
6.9 Severinghaus carbon dioxide electrode . . . 217
6.10 Temperature measurement . . . 218
6.11 Thermocouple and Seebeck effect . . . 219

SECTION 7 EQUIPMENT

7.1 Bag valve mask resuscitator . . . 221
7.2 Breathing circuits – circle system . . . 222
7.3 Breathing circuits – Mapleson's classification . . . 223
7.4 Cleaning and decontamination . . . 224
7.5 Continuous renal replacement therapy – extracorporeal circuit . . . 225
7.6 Continuous renal replacement therapy – modes . . . 226
7.7 Gas cylinders . . . 227
7.8 Humidifier . . . 228
7.9 Oxygen delivery systems – Bernoulli principle and Venturi effect . . . 229
7.10 Piped gases . . . 230

7.11 Scavenging 231
7.12 Vacuum-insulated evaporator 232
7.13 Vaporizer 233
7.14 Ventilation – pressure-controlled 234
7.15 Ventilation – volume-controlled 235

SECTION 8 STATISTICS

8.1 Mean, median and mode 237
8.2 Normal distribution 238
8.3 Number needed to treat 239
8.4 Odds ratio 240
8.5 Predictive values 241
8.6 Sensitivity and specificity 242
8.7 Significance tests 243
8.8 Statistical variability 244
8.9 Type I and type II errors 245

Preface

This book is a compendium of the diagrams, graphs, equations and tables needed for anaesthetic practice. It has been written with the FRCA examinations in mind, although it is equally well suited for revision at any stage of an anaesthetic practitioner's career. Senior anaesthetists will find this book useful as an aide-memoire when teaching and examining trainee colleagues. Additionally it is hoped it will prove useful to anyone who is looking for short and clear explanations of the fundamental principles surrounding anaesthesia.

Each page contains a separate topic with the relevant diagram, graph, equation or table succinctly described for rapid review and assimilation. The diagrams and graphs have been specifically drawn to allow them, in the main, to be easily reproduced in an exam setting. Additionally, a simple standardized colour palette has been used throughout the book to allow anyone with a 4-colour pen to draw the diagrams clearly and accurately.

The explanations are purposely short (250–300 words) but have been carefully written to provide enough up to date detail to effectively explain the illustration, equation, graph or table. Although the text is centred on an explanation of the basic sciences related to the topic, where appropriate the clinical applications of the principles are also discussed.

Many anaesthetic textbooks have good diagrams and detailed explanations but few, if any, have all the diagrams needed for anaesthetic practice and the FRCA examinations. This book has been borne out of that need and we hope you will find it useful and stimulating.

Tim Hooper, James Nickells, Sonja Payne,
Annabel Pearson and Ben Walton

June 2015

About the authors

The idea for the book was that of lead author Tim Hooper, Army anaesthetist, intensivist and prehospital care doctor. Experienced writer, artist and anaesthetist James Nickells provided original artwork for the book, while anaesthetist and intensivist Ben Walton used his considerable writing experience to help edit it. Senior anaesthetic trainees Sonja Payne and Annabel Pearson had the unenviable task of researching and writing each topic and without them this book would still be only an idea. All authors work and live in the Bristol region.

Abbreviations

AAG	α-1-acid glycoprotein
ACA	anterior cerebral artery
ACE	angiotensin converting enzyme
ACh	acetylcholine
ACOM	anterior communicating artery
ADH	antidiuretic hormone
ANP	atrial natriuretic peptide
ANS	autonomic nervous system
APL	adjustable pressure limiting
ARDS	acute respiratory distress syndrome
ARR	absolute risk reduction
ATP	adenosine triphosphate
AV	atrioventricular
BVM	bag valve mask
CBF	cerebral blood flow
CC	closing capacity
CI	confidence interval
CMR	central metabolic rate
CMV	controlled mechanical ventilation
CNS	central nervous system
CO	cardiac output
COPD	chronic obstructive pulmonary disease
CPP	cerebral perfusion pressure
CRRT	continuous renal replacement therapy
CSF	cerebrospinal fluid
CV	closing volume
CVP	central venous pressure
CVVH	continuous veno-venous haemofiltration
CVVHD	continuous veno-venous haemodialysis
CVVHDF	continuous veno-venous haemodiafiltration
DBS	double-burst stimulation
DCT	distal convoluted tubule
ECF	extracellular fluid
ECG	electrocardiogram
EDPVR	end-diastolic pressure–volume relationship
EDV	end-diastolic volume
EMI	electromagnetic interference
ERAD	extreme right axis deviation
ERV	expiratory reserve volume
ESPVR	end-systolic pressure–volume relationship
ESV	end-systolic volume
FEF	forced expiratory flow
FEV1	forced expiratory volume in 1 second
FGF	fresh gas flow
FICB	fascia iliaca compartment block
FNB	femoral nerve blockade
FRC	functional residual capacity
FVC	forced vital capacity
GFR	glomerular filtration rate
GI	gastrointestinal
GPCR	G-protein couple receptor
GTO	Golgi tendon organ
Hb	haemoglobin
IA	intrinsic activity
IC	inspiratory capacity
ICA	internal carotid artery
ICD	implantable cardioverter-defibrillator
ICF	intracellular fluid
ICP	intracranial pressure
IQR	interquartile range
IRV	inspiratory reserve volume
ISF	interstitial fluid
IVC	inferior vena cava
$IV_{ol}C$	isovolumetric contraction
$IV_{ol}R$	isovolumetric relaxation
LAP	left atrial pressure

LBBB	left bundle branch block
LCNT	lateral cutaneous nerve of the thigh
MAC	membrane attack complex
MAC	minimum alveolar concentration
MAP	mean arterial pressure
MBL	mannose-binding lectin
MCA	middle cerebral artery
MPAP	mean pulmonary artery pressure
M_v	minute ventilation
NADH	nicotinamide adenine dinucleotide
NMB	neuromuscular blockade
NMBD	neuromuscular blocking drug
NMJ	neuromuscular junction
NNH	number needed to harm
NNT	number needed to treat
NPV	negative predictive value
NSAIDs	non-steroidal anti-inflammatory drugs
OR	odds ratio
PAH	pulmonary arterial hypertension
PCA	posterior cerebral artery
PCOM	posterior communicating artery
PCV	pressure-controlled ventilation
PCV–VG	pressure-controlled ventilation with volume guarantee
PCWP	pulmonary capillary wedge pressure
PEEP	positive end-expiratory pressure
PEFR	peak expiratory flow rate
PNS	peripheral nervous system
PPV	positive predictive value
PRT	platinum resistance thermometer
PVR	pulmonary vascular resistance
RA	right atrium
RAD	right axis deviation
RBBB	right bundle branch block
RBF	renal blood flow
RLN	recurrent laryngeal nerve
RMP	resting membrane potential
RR	relative risk
RTD	resistance temperature detector
RV	residual volume
SA	sinoatrial
SBE	standardized base excess
SCM	sternocleidomastoid
SCUF	slow continuous ultrafiltration
SD	standard deviation
SID	strong ion difference
SLN	superficial laryngeal nerve
SNS	sympathetic nervous system
STP	standard temperature and pressure
SV	spontaneous ventilation
SV	stroke volume
SVP	saturation vapour pressure
SVR	systemic vascular resistance
SVT	supraventricular tachycardia
TBW	total body water
TCI	target controlled infusion
TEB	thoracic electrical bioimpedance
TENS	transcutaneous electrical nerve stimulation
TIVA	total intravenous anaesthesia
TLC	total lung capacity
TMP	transmembrane pressure
TOF	train of four
TPN	total parenteral nutrition
TV	tidal volume
VC	vital capacity
VCV	volume-controlled ventilation
VGCC	voltage-gated calcium channels
VIE	vacuum-insulated evaporator
vWF	von Willebrand factor

1.1.1

Cardiac action potential – contractile cells

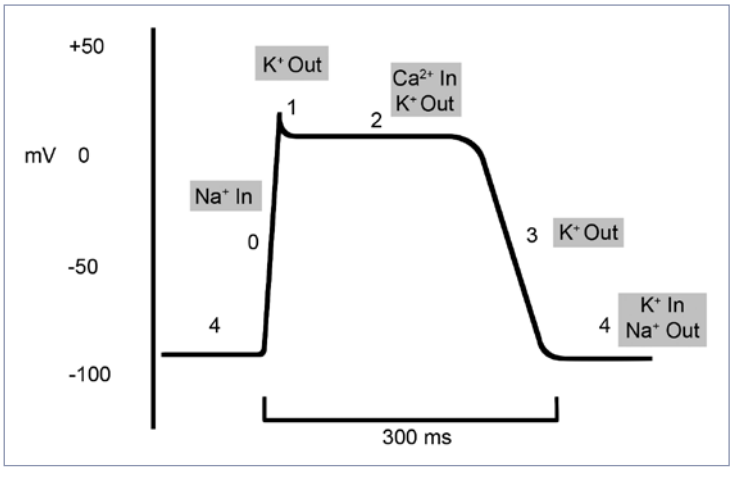

The cardiac action potential differs significantly depending on the function of the cardiac myocyte (i.e. excitatory/pacemaker or contractile). The action potential of contractile cardiac myocytes has 5 phases characterized by a stable resting membrane potential and a prolonged plateau phase.

- Phase 0 – rapid depolarization as membrane permeability to potassium decreases and fast sodium channels open.
- Phase 1 – early rapid repolarization as sodium permeability decreases.
- Phase 2 – plateau phase. A continued influx of calcium through L-type (long opening, voltage-gated) calcium channels maintains depolarization for approximately 300 ms.
- Phase 3 – rapid repolarization due to inactivation of calcium channels and ongoing efflux of potassium.
- Phase 4 – restoration of ionic concentrations, thereby restoring the resting membrane potential of approximately –90 mV.

For the majority of the action potential, contractile myocytes demonstrate an absolute refractory period (beginning of phase 0 until close to end of phase 2). During this time no stimulus, regardless of the magnitude, can incite further depolarization. A relative refractory period exists during phase 3. A supramaximal stimulus during this period will result in an action potential with a slower rate of depolarization and smaller amplitude, producing a weaker contraction.

Anti-arrhythmic drugs and the myocardial action potential

Anti-arrhythmic drugs (see *Section 1.1.22 – Vaughan–Williams classification*) that alter ion movement are used to alter action potentials to prevent or terminate arrhythmias.

- In contractile cells, sodium channel blockers (Vaughan–Williams Class 1) reduce the slope of phase 0 and the magnitude of depolarization. They also prolong the refractory periods by delaying the reactivation of sodium channels.
- Potassium channel blockers (Vaughan–Williams Class 3) delay phase 3 repolarization. This lengthens the duration of the action potential and the refractory periods.

1.1.2

Cardiac action potential – pacemaker cells

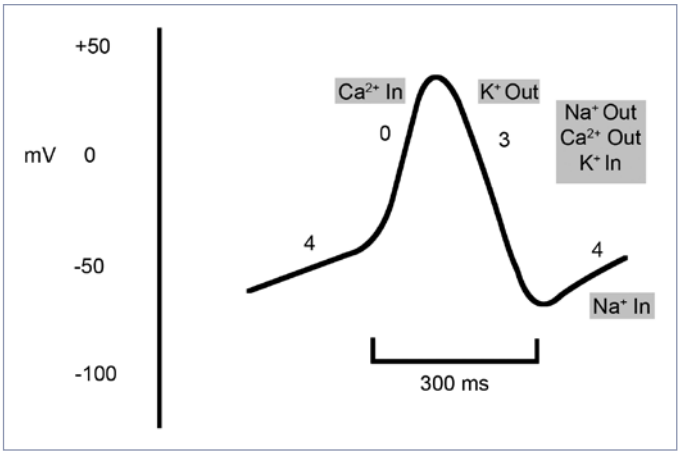

The pacemaker potential is seen in cells of the cardiac excitatory system, namely the sinoatrial (SA) and atrioventricular (AV) nodes. Action potentials of cardiac pacemaker myocytes have 3 phases (named out of numerical order to coincide with contractile myocyte action potentials) and are characterized by automaticity, due to an unstable phase 4, and a lack of plateau phase.

- Phase 4 – spontaneous depolarization. Sodium moves into myocytes via 'funny' voltage-gated channels that open when the cell membrane potential becomes more negative, immediately after the end of the previous action potential. Calcium also enters the cell via T-type channels (T for transient).
- Phase 0 – rapid depolarization occurs once the threshold potential (approximately –40 mV) is reached. L-type calcium channels open and calcium enters the cell.
- Phase 3 – repolarization occurs as potassium permeability increases, resulting in potassium efflux.

Compared to contractile myocytes, pacemaker myocyte action potentials:

- are slow response
- have a less negative phase 4 membrane potential
- have a less negative threshold potential
- have a less steep slope of rapid depolarization (phase 0).

Regulation by the autonomic nervous system

The cardiac excitatory system demonstrates inherent pacemaker activity. The rate of depolarization and duration of action potential are influenced by the autonomic nervous system. In the denervated heart, the SA node depolarizes at a rate of 100 bpm. At rest, parasympathetic activity dominates and reduces SA nodal depolarization. Parasympathetic activation leads to an increase in potassium efflux while reducing sodium and calcium influx. These alterations in ionic conductance result in a more negative phase 4 membrane potential, a decrease in the slope of phase 4 and, overall, an increase in the time to reach the threshold potential. Conversely, sympathetic activation increases the rate of pacemaker depolarization by reducing potassium efflux and increasing sodium and calcium influx.

1.1.3

Cardiac action potential – variation in pacemaker potential

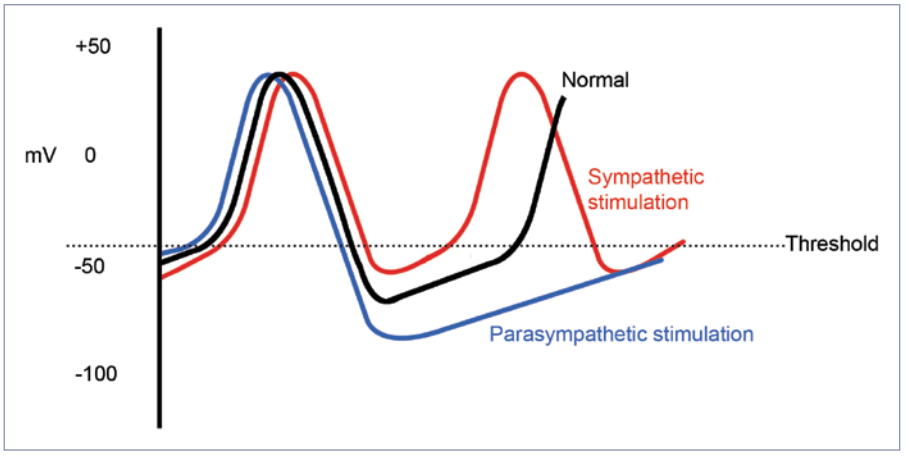

The pacemaker potential is seen in cells in the SA and AV nodes. It is a slow positive increase from the resting potential that occurs at the end of one action potential and before the start of the next. The pacemaker action potential differs from those seen in other cardiac cells because it lacks phases 1 and 2 and has an unstable resting potential. This unstable resting potential allows for spontaneous depolarization and gives the heart its autorhythmicity. It is the rate of change, or gradient, of the resting potential that determines the onset of the next action potential and therefore the discharge rate. The characteristics of the pacemaker potential are predominantly under the control of the autonomic nervous system.

An increase in the gradient of the slope of phase 4 will reduce the amount of time taken for the cell to reach threshold potential, causing depolarization to occur more rapidly. This occurs with sympathetic stimulation (red trace) via β1 adrenoreceptors which results in an increase in cyclic-AMP levels, allowing the opening of calcium channels and thereby increasing the discharge rate of the cell.

Conversely, a decrease in the slope of phase 4 will increase the time taken to reach threshold potential and depolarization, causing a reduced discharge rate. This occurs with parasympathetic stimulation (blue trace). The vagus nerve acts to slow the discharge rate by hyperpolarizing the cell membrane through increased permeability to potassium. The membrane potential is therefore more negative so will take longer to reach threshold potential and to discharge.

1.1.4
Cardiac cycle

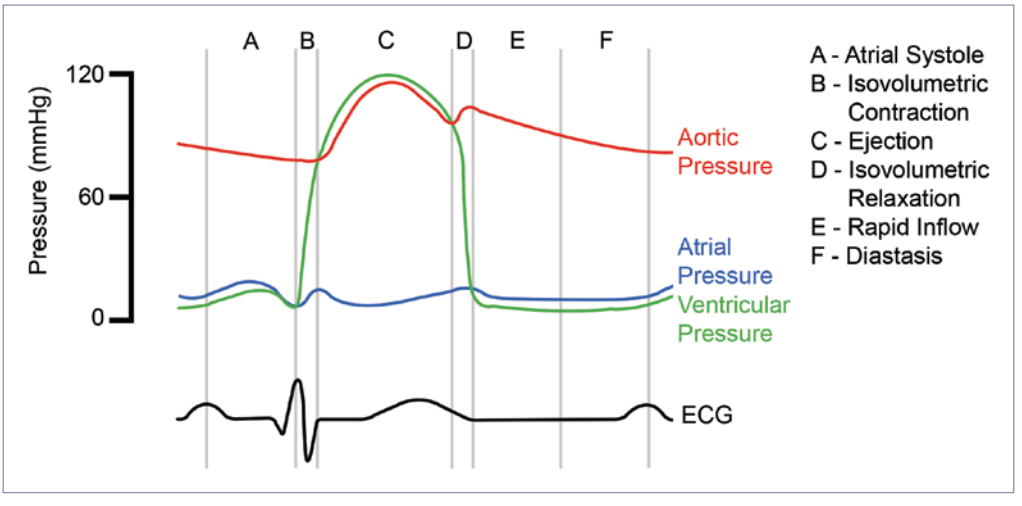

The diagram depicts events that occur during one cardiac cycle. It is a graph of pressure against time and includes pressure waveforms for the left ventricle, aorta and central venous pressure (CVP), with the electrocardiogram (ECG) and heart sound timings superimposed.

There are five phases.

- Phase 1 (A). Atrial contraction – 'P' wave of the ECG and 'a' wave of the CVP trace. Atrial contraction (or 'atrial kick') contributes to about 30% of ventricular filling.
- Phase 2 (B). Ventricular isovolumetric contraction ($IV_{ol}C$) – marks the onset of systole and coincides with closure of the mitral and tricuspid valves (first heart sound). The pressure in the ventricle rises rapidly from its baseline, while blood volume remains constant, since both inlet and outlet valves are closed. The 'c' wave of the CVP trace represents tricuspid valve bulging as the right ventricle undergoes $IV_{ol}C$.
- Phase 3 (C). Systole – as the ventricular pressure exceeds that in the aorta and pulmonary arteries, the aortic and pulmonary valves open and blood is ejected. The aortic pressure curve follows that of the left ventricle, but at a slightly lower pressure, depicting the pressure gradient needed to allow forward flow of blood. At the end of this phase, ventricular repolarization is represented by the 't' wave on the ECG.
- Phase 4 (D). Ventricular isovolumetric relaxation ($IV_{ol}R$) – once the aortic and pulmonary valves close (second heart sound), the ventricular pressure rapidly falls to baseline with no change in volume. Aortic valve closure is seen on the aortic pressure trace as the dicrotic notch, after which the pressure in the aorta exceeds that in the ventricle.
- Phase 5 (E and F). Ventricular filling – passive filling of the ventricle during diastole. As ventricular pressure falls below atrial pressure (and CVP), the tricuspid and mitral valves open allowing forward flow of blood. This filling is initially rapid (E), followed by a slower filling phase known as diastasis (F), before atrial contraction occurs and the cycle starts again. The 'y' descent on the CVP trace occurs as the atrium empties.

1.1.5
Cardiac output equation

$$Q = HR \times SV$$

Q = cardiac output ($ml.min^{-1}$)

HR = heart rate ($beats.min^{-1}$)

SV = stroke volume ($ml.beat^{-1}$)

Cardiac output (CO) is defined as volume of blood pumped by the heart per minute; it is equal to the product of heart rate and stroke volume. In considering this equation there are four determinants of CO: heart rate, preload, afterload and contractility. Changes in each variable do not occur in isolation but will impact the remaining variables. Therefore, depending on the magnitude of change, each variable may positively or negatively impact CO.

CO monitoring is frequently used as a means of optimizing tissue oxygenation and guiding treatment. Historically, the gold standard for CO measurement was invasive pulmonary artery catheterization. However, due to the specialist skill required for insertion and the potential for complications, its use has been superseded by less invasive methods.

- Pulse contour analysis (i.e. PiCCO, LiDCO) – algorithms relate the contour of the arterial pressure waveform to stroke volume and systemic vascular resistance. Research demonstrates good agreement with the gold standard. Limitations include the necessity for an optimal arterial pressure trace and potential for error (arrhythmias, aortic regurgitation).
- Oesophageal Doppler – estimates CO through measurement of blood velocity in the descending aorta (see *Section 5.5 – Doppler effect*).
- Transpulmonary thermodilution – based on the classical dilution method (dilution of known concentration of indicator injectate is measured within the arterial system over time) and is coupled with pulse contour analysis in the PiCCO system. Thermodilution is utilized to calibrate the PiCCO system and to provide measurements of volumetric parameters (i.e. global end-diastolic index) and extravascular lung water.
- Thoracic electrical bioimpedance (TEB) – a small electrical current is passed through electrodes applied to the neck and chest. The pulsatile flow of blood leads to fluctuations in current allowing calculation of CO from the impedance waveform. Studies have shown poor correlation between CO values derived via TEB and those dervived via thermodilution methods.

1.1.6
Central venous pressure waveform

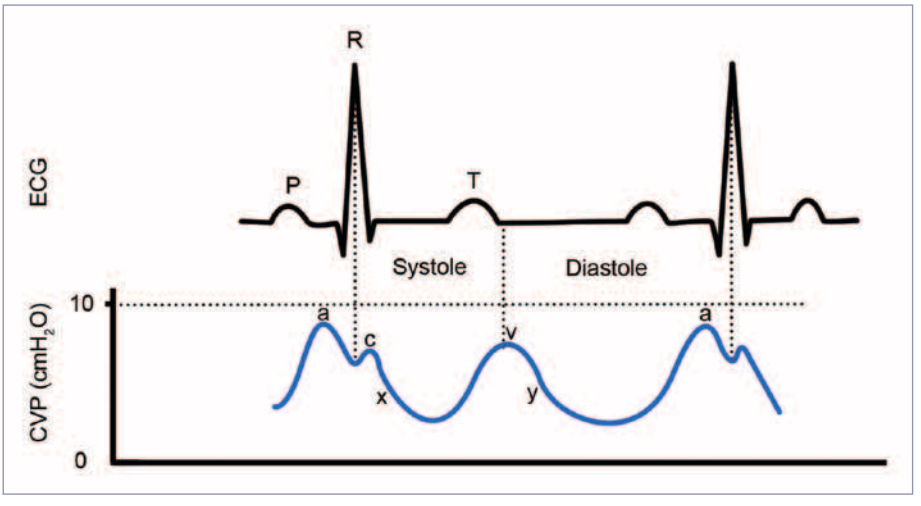

The central venous pressure (CVP) waveform reflects the pressure at the junction of the vena cavae and the right atrium. It consists of three peaks and two descents:

- 'a wave' – the most prominent wave, represents right atrial contraction
- 'c wave' – interrupts 'a wave' decline, due to bulging of the tricuspid valve into the right atrium during right ventricular isovolumetric contraction ($IV_{ol}C$)
- 'x descent' – decline of right atrial pressure during ongoing right ventricular contraction
- 'v wave' – increase in right atrial pressure due to venous filling of the right atrium during late systole
- 'y descent' – decline of right atrial pressure as the tricuspid valve opens.

Alignment with the ECG trace may aid identification of the CVP waveform components.

- Onset of systole marked by ECG R wave; onset of diastole marked by end of ECG T wave.
- Three systolic components – 'c wave', 'x descent' and 'v wave'.
- Two diastolic components – 'y descent' and 'a wave'.

Potential errors in CVP measurement

Sampling errors: positioning of both the central venous catheter and the pressure transducer are important for accurate and precise measurement. Due to the narrow clinical range of CVP, small variations in the transducer reference point may have a disproportionally large effect on CVP measurement.

Interpretation errors: the effects of ventilation on CVP measurement must be considered. All vascular pressures should be measured at end-expiration, because pleural pressure is closest to atmospheric pressure. In positive pressure ventilation, low PEEP results in minimal error by only increasing the observed value by 1–2 mmHg. With high PEEP, error may be more difficult to predict.

1.1.7

Central venous pressure waveform – abnormalities

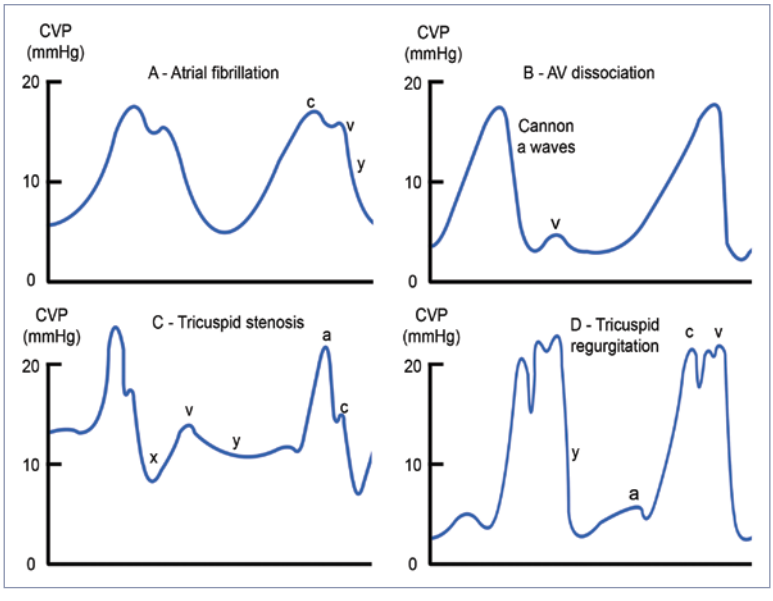

Examination of the CVP waveform may aid diagnosis of various pathophysiological conditions.

Cardiac arrhythmias

A – Atrial fibrillation is characterized by an absent 'a wave'. The 'c wave' is more prominent due to a greater than normal right atrial volume at the end of diastole.

B – In isorhythmic AV dissociation, the atria and ventricles beat independently of each other but at the same rate. As such, the atria contract against a closed tricuspid valve producing an enlarged 'a wave' termed a 'cannon a wave'.

Other arrhythmias also affect the CVP waveform. Sinus tachycardia is characterized by a shortening of diastole and therefore alters the diastolic waveform components (shortening of 'y descent' with merger of the 'v' and 'a' waves). In contrast, sinus bradycardia leads to increased distinction between the three waves.

Valvular disease

C – Tricuspid stenosis is a diastolic abnormality impeding right atrial emptying. As the right atrium contracts against a narrowed tricuspid valve, a prominent 'a wave' is produced. Right atrial pressure remains elevated for longer than normal, attenuating the 'y descent'.

D – In tricuspid regurgitation, systolic flow of blood back into the right atrium through an incompetent valve leads to a persistent elevation of right atrial pressure. As such, the 'c' and 'v' waves gradually merge over time with subsequent loss of the 'x descent'.

Elevation of CVP may be observed with raised intrathoracic pressure (positive-pressure ventilation), cardiac dysfunction (cardiac tamponade, cardiac failure) and circulatory overload.

Reduction in CVP may occur in association with reduced venous return (hypovolaemia, vasodilatation) and a reduction in intrathoracic pressure (spontaneous inspiration).

1.1.8
Einthoven triangle

Bipolar leads (I, II, III) electrically form an equilateral triangle named after Willem Einthoven, the scientist who developed the ECG. These leads, combined with unipolar augmented leads (aVL, aVR, aVF) examine the heart in the frontal plane. Rearranging these six limb leads, allowing an intersection representing the heart, forms the hexaxial reference system. The arrows represent the normal path of electrical current for each lead. This graphical representation of cardiac electrical activity aids interpretation of ventricular axis in the frontal plane.

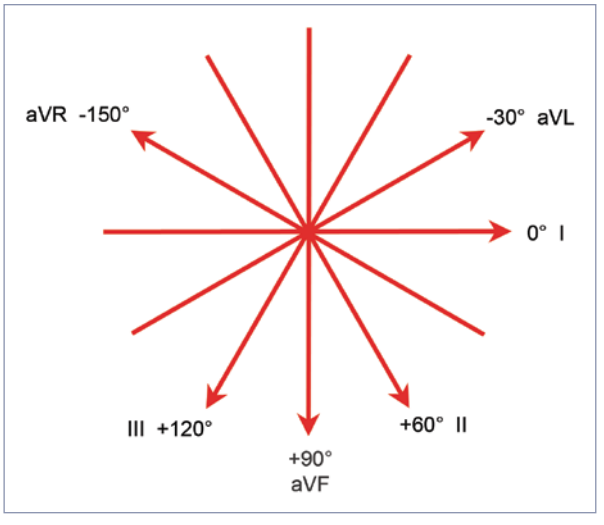

Frontal ventricular axis determination

Normal cardiac electrical activity progresses systematically from the SA node, via internodal fibres to the AV node. Conduction continues via the bundle of His, through right and left bundle branches to Purkinje fibres, resulting in ventricular contraction. Depolarization towards a positive electrode produces a positive deflection on the ECG. When viewing the heart in the frontal plane, mean ventricular depolarization (as denoted by the QRS complex) lies between –30° and +90°. Ventricular axis may be determined using the limb leads. The simplest approach is the quadrant method, examining leads I and aVF. These perpendicular limb leads outline the majority of the normal axis.

- Normal axis – positive QRS complex in both leads.
- Extreme right axis deviation – negative QRS complex in both leads.
- Right axis deviation – negative complex in lead I, positive complex in aVF.
- Left axis deviation – positive complex in lead I, negative complex in aVF. However, as the normal axis ranges from –30° to +90°, this average vector may represent a normal axis. Examination of lead II is also required; if QRS complex is positive the axis is normal (ranging from 0° to –30°).

An alternative equiphasic approach exists, founded on the principle that depolarization travelling perpendicular to a lead produces an equiphasic QRS complex.

1.1.9
Ejection fraction equation

$$EF = \frac{SV}{EDV} \times 100$$

$$SV = EDV - ESV$$

EF = ejection fraction

EDV = end-diastolic volume

ESV = end-systolic volume

SV = stroke volume

The ejection fraction simply describes the amount of blood that is ejected from the ventricle during systolic contraction (stroke volume) as a proportion of the amount of blood that is present in the ventricle at the end of diastole (end-diastolic volume). A 70 kg individual would normally have a stroke volume of about 70 ml and an end-diastolic volume of about 120 ml.

The ejection fraction equation is used to calculate the stroke volume as a percentage of the end-diastolic volume. It gives an indication of the percentage of the ventricular volume that is ejected during each systolic contraction. It can be applied to the left or the right ventricles, with normal values being 50–65%. Right and left ventricular volumes are roughly equal and therefore ejection fractions are broadly similar.

In clinical practice, it can be calculated using echocardiography, pulmonary artery catheterization, nuclear cardiology or by contrast angiography.

In aortic stenosis, the ventricle will compensate for the increased obstruction to outflow by hypertrophy. This will initially maintain the ejection fraction and the pressure gradient across the valve. As the disease progresses and the valve area narrows, the hypertrophied ventricle becomes stiff and less compliant and will no longer be able to compensate. A reduction in the stroke volume (and ejection fraction) is seen, resulting in a fixed reduced cardiac output. The myocardium will eventually fail as compliance continues to worsen.

1.1.10 Electrocardiogram

An electrocardiogram (ECG) is a non-invasive, transthoracic interpretation of cardiac electrical activity over time. Thorough assessment requires a systematic approach including rate, rhythm, axis (normal axis is –30° to +90°), and wave morphology/interval.

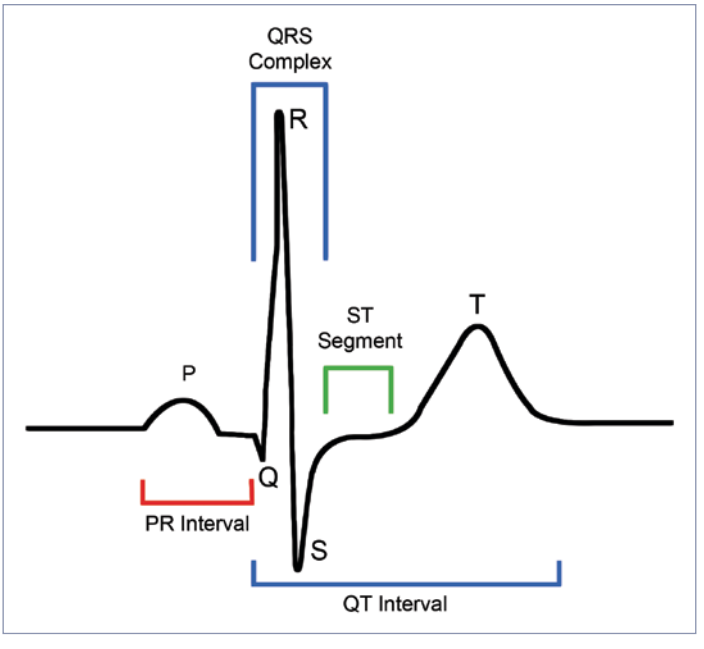

Morphology and intervals

- P wave – represents atrial depolarization. A positive deflection should be present in all leads except aVR.
- PR interval – from the start of the P wave to the end of the PR segment. Normal value 0.12–0.2 s (3–5 small squares). This interval is rate dependent; as heart rate increases, the PR interval decreases.
- QRS wave – represents ventricular depolarization. The normal duration is ≤0.12 s. A Q wave in leads V1–V3 is abnormal.
- ST segment – from the junction of the QRS complex and the ST segment to the beginning of the T wave. A normal ST segment is isoelectric.
- T wave – represents repolarization of the ventricles.
- QT interval – from the start of the QRS complex to the end of the T wave. This interval represents the time for ventricular activation and recovery. Heart rate variability occurs and therefore a corrected QT interval (QTc) can be calculated (normal value is <0.44 s).

ECG changes associated with acute coronary syndromes and myocardial infarction

- Acute coronary syndromes – include non-ST-elevation myocardial infarction and unstable angina. The primary ECG changes observed are ST segment depression and T wave flattening or inversion.
- Myocardial infarction – early evidence of transmural ischaemia and myocardial infarction includes hyperacute T waves followed by ST elevation. Q wave formation may begin within 1 hour of infarction. Inverted T waves are a later sign within 72 hours of cell death. Stabilization of the ST segment usually occurs within 12 hours, although ST elevation may persist for more than 2 weeks.

1.1.11

Electrocardiogram – cardiac axis and QTc

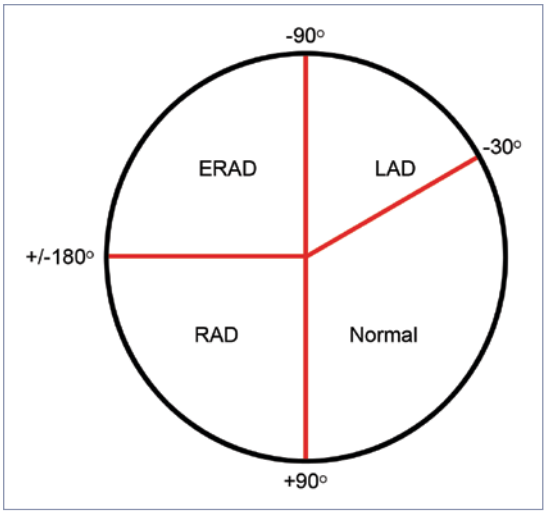

Division of the hexaxial reference system into four quadrants allows further interpretation of the cardiac ventricular axis (for calculation see *Section 1.1.8 – Einthoven triangle*).

- The normal QRS axis ranges from –30° of left axis deviation (LAD) to +90°.
- LAD is defined as an axis between –30° and –90°. This may be an isolated finding or can be associated with pathology. Causes include: left ventricular hypertrophy, left bundle branch block (LBBB), left anterior fascicular block, myocardial infarction, and mechanical shifts of the heart (i.e. pneumothorax).
- Right axis deviation (RAD) is defined as an axis between +90° and +180°. Causes include: physiological variant in infants and children, right ventricular hypertrophy, myocardial infarction, left posterior fascicular block, chronic lung disease, dextrocardia, and ventricular arrhythmias.
- Extreme right axis deviation (ERAD) is defined as an axis of –90° to +180°. This is a rare finding associated with dextrocardia, ventricular arrhythmias or a paced rhythm.

Precordial axis

Assessment of the precordial leads, V1–V6, enables determination of the precordial axis as described by R wave progression. Normal R wave progression is characterized by a primarily negative QRS complex in V1 and a primarily positive QRS complex in V6. Transition between negative and positive complexes occurs between the V2 and V4 leads.

- Early R wave progression is characterized by much more positive QRS complexes in leads V1 and V2. This observation is always pathological and may be due to posterior myocardial infarction (with the positive QRS complexes representing reciprocal Q waves), right ventricular hypertrophy, RBBB, or Wolff–Parkinson–White syndrome.
- Poor R wave progression is characterized by a predominance of negative QRS complexes through the transitional precordial leads. This late transition can be a normal variant but may also be associated with anterior myocardial infarction, left ventricular hypertrophy, LBBB, or lung disease.